Available online at www.sciencedirect.com
SCIENCE DIRECT®
International Journal of Multiphase Flow 31 (2005) 318–336
International Journal of Multiphase Flow
www.elsevier.com/locate/ijmulflow

Characteristics of fiber suspension flow in a rectangular channel

Hanjiang (John) Xu [a], Cyrus K. Aidun [b,*]

[a] *Corporate Technology, International Paper, Loveland, OH, United States*
[b] *School of Mechanical Engineering, Georgia Institute of Technology, 500, 10th Street NW, Atlanta, GA 30332, United States*

Received 13 July 2004; received in revised form 17 December 2004

Abstract

Velocity profile of fiber suspension flow in a rectangular channel is measured by pulsed ultrasonic Doppler velocimetry (PUDV), and the effect of fiber concentration and Reynolds number on the shape of the velocity profile is investigated. Five types of flow behavior are observed when fiber concentration increases or flow rate decreases progressively. The turbulent velocity profiles of fiber suspension can be described by a correlation with fiber concentration, nl^3, and Reynolds number, Re as the main parameters. The presence of fiber in the suspension will reduce the turbulence intensity and thus reduce the turbulent momentum transfer. On the other hand, fibers in the suspension have the tendency to form fiber networks, which will increase the momentum transfer. The relative contribution of these two types of momentum flux will determine the final shape of the velocity profile.

Keywords: Fiber suspension; Pulsed ultrasonic Doppler velocimetry; Flow mechanism; Velocity profile

* Corresponding author. Tel.: +1 404 894 6645; fax: +1 404 894 4778.
E-mail address: cyrus.aidun@me.gatech.edu (C.K. Aidun).

0301-9322/$ - see front matter © 2005 Elsevier Ltd. All rights reserved.
doi:10.1016/j.ijmultiphaseflow.2004.12.003

1. Introduction

Many industrial processes involve flow of fiber suspension in channels and pipes with various size and shape. In the paper manufacturing industry, for example, flow of dilute to concentrated fiber suspension takes place in circular pipes, straight and converging channels. The properties of the final product often depend on the flow characteristics, such as the velocity profile and the wall shear stress. In order to understand the flow characteristics, it is important to know the effect of fiber concentration and flow rate on the velocity profile. Because there is limited optical access in fiber suspension flows, particularly in the non-dilute regime, velocity profile measurements are not trivial. Because fibers tend to staple on the probe surface and lack of optical access, techniques developed for velocity measurements in single-phase flows, such as laser Doppler velocimetry (LDV) and hot-wire anemometry are generally not effective. Even in the dilute wood fiber suspension, it is found that the penetration depth of LDV measurements is severely limited because of the light-scattering properties of wood fibers (Kerekes and Garner, 1982).

In their studies of fiber suspension flow, Forgacs et al. (1958) and Daily and Bugliarello (1958) showed three basic types of flow regime, namely plug, mixed, and turbulent flow. At low flow rates, a plug region exists in which the core is a coherent plug of fiber network with no movement of the fibers relative to one another. Outside the plug, there is essentially fiber-free water annulus near the wall. These investigators explain that at higher flow rate, in the mixed flow regime, the turbulent stress becomes higher than the yield stress of fiber network, resulting in progressive disintegration of the plug. In this mixed flow regime, there is turbulent-like flow near the wall and plug-like flow at the center of the flow field. With further increases in flow rate, the entire fiber network will be broken and the flow becomes turbulent across the entire cross-section of the channel. Some early experiments by Daily and Bugliarello (1958), using a special impact probe with a wide flat-faced tip, to prevent clogging of fibers, show that the velocity profile in a pipe flow becomes 'sharper' (less blunt) with an increase in flow rate. Also, for a specified range of fiber concentration and mean velocity, the velocity profile becomes blunter as concentration increases. Using an annular purge impact tube, Mih and Parker (1967) measured the local mean velocities for the turbulent fiber suspension flow in a pipe and found that, at low turbulent flow rates, a central plug region will develop. This plug region shrinks as the flow rate increases, and perhaps finally vanishes. In the turbulent flow regime, they found that the profile appears to be similar to single phase flow. They found that the apparent von Kármán constant (defined as the inverse of slope of the velocity profile in a semi-log coordinate, see Eq. (2) below) is lower for the fiber suspensions than for single phase Newtonian fluids, and varies with fiber concentration. In contradiction to results by Mih and Parker (1967), using the same measurement technique, Seely (1968) found that the von Kármán constant increases in a systematic manner throughout the damped turbulent regime and approaches the single phase Newtonian value ($\sim$0.41) at high flow rates. Sanders and Meyer (1971) report that the von Kármán constant decreases with increasing concentration and decreasing flow rate. By the similar purge impact tube, Lee and Duffy (1976) investigated the velocity profiles of fiber suspension over a wide range of bulk velocities. They found that the fully turbulent velocity profiles become steeper as fiber concentration increases. The reduced local velocity (u^+ as defined in the next section) for fiber suspension in the turbulent flow regime is greater than that of single

phase flow, such as water, under the same conditions. In the low flow rate turbulent regime, the von Kármán constant decreases with the flow rate, while at high flow rate regime the behavior is reversed.

During the last twenty years, different methods have been used to study the flow behavior of fiber suspension. Of the non-intrusive techniques, NMR imaging has been demonstrated to be an effective tool for measurement of the mean velocity profile of cellulose fibers suspended in water. Li et al. (1994) and Powell et al. (1996) used this technique to measure the average velocity of fiber suspension flow at flow rates up to 1 m/s. They show that, at the flow rates and concentrations studied, the suspension undergo mixed flow in which there is plug in the center of tube and a high shear region near the wall. The size of the plug decreases as the mean flow rate increases. However, because of the limitation of NMR technique, it is very hard to obtain the velocity profile of suspension flow at higher flow rates.

Using an LDV system, Steen (1989) measured the mean velocity and turbulent fluctuations in glass fiber suspension flow in a pipe by matching the index of refraction in a mixture of ethanol and benzyl alcohol. He measured the mean and fluctuating components of velocity and the turbulence spectra with glass fiber concentration of 1.2 and 12 g/l in ethanol and benzyl alcohol. His measurements show that turbulent intensity increases with the decreasing of fiber concentration and fiber length. With the same index-matching technique, Andersson and Rasmuson (2000) studied the transition of fiber suspension to turbulent flow in a rotary shear tester and found that the fluctuation velocity approaches that of single-phase flow with increasing rotational speed. In their experiments, they used glass fibers with 9 μm diameter and 1.5 and 3 mm lengths. The fiber concentration was varied from 3% to 20% by weight in ethanol benzyl having a density ratio 2.4 (2475/1022).

In addition to the change of velocity profile and turbulence intensity, another characteristic of fiber suspension flow is the non-uniform distribution of fiber concentration in the flow field. In an early study by Sanders and Meyer (1971), it was found that the concentration increases from the wall to the center of the pipe. This behavior is in agreement with the behavior of particulate flow in pipes and channels where particles migrate from the higher shear region near the wall to the lower shear region near the center (see for example Hookham, 1986, and Koh et al., 1994, who used a modified laser-Doppler technique to measure the velocity and concentration profiles for the flow of concentrated suspensions in a rectangular channel). It is found that the concentration becomes more uniform with increasing flow rate and with decreasing the average concentration. Olson (1996) investigated the distribution of fiber concentration for a range of fiber lengths in a channel flow. In his study, the fiber concentration is less than 5000 fibers/l, so that the fiber–fiber interaction is negligible. He shows that the variations in concentration show a linear region near the wall and an almost constant region above a height of about half fiber length from the wall. A maximum peak between the linear and constant concentration regions is observed.

The rheology of fiber suspension including the bulk stress in a suspension of rigid rods (Batchelor, 1970, 1971; Hinch and Leal, 1976; Shaqfeh and Fredrickson, 1990), the orientation distribution of fibers (Shaqfeh and Koch, 1988; Rahnama et al., 1995), the effective viscosity of the fiber suspension (Batchelor, 1971; Hinch and Leal, 1976; Shaqfeh and Fredrickson, 1990; Yamamoto and Matsuoka, 1994), and the particle concentration profile in the flow (Kallio and Reeks, 1989; Kroger and Drossinos, 2000; Dong et al., 2003) have been investigated. How-

ever, the above analyses of fibers or slender rods are limited to infinite dilution or semi-dilute concentrations. The former completely neglects fiber–fiber interactions and therefore requires $nl^3 \ll 1$, where n is fiber number density and l is fiber half-length. The latter accounts for interactions among the fibers and assumes $nl^3 \gg 1$ and $\phi \ll 1$, where ϕ is the volume fraction of the fiber materials. Although some of the simple properties of fiber suspension (e.g., viscosity) can be predicted from theoretical analyses, it is very difficult to model the velocity profile of fiber suspension flow, especially in the concentrated fiber suspension regime where fiber network formation, non-uniform distribution of fibers in the flow field, variations in effective viscosity, and fiber deformation are considered.

Because of the entanglement of fiber and subsequent floc formation, it is difficult to obtain the velocity profile of fiber suspension at higher concentrations using existing traditional techniques. Some inconsistent results on how fibers affect the velocity profile of fiber suspension flow have been reported. To clarify the discrepancies in the velocity profile data reported in the literature, pulsed Doppler ultrasonic velocimetry (PUDV) is used in this study to measure the velocity profile of fiber suspension flow in a rectangular channel. This technique is based on the echography for position information and Doppler shift relationships for velocity detection (Takeda, 1986). During the measurement, an ultrasound pulse is emitted from the transducer along the measuring line, and the same transducer receives the echo reflected from the surface of particles suspended in the liquid. Information on the position from which the ultrasound is reflected can be extracted from the time delay after the start of the pulse burst. The instantaneous velocity information is derived from the Doppler shift. Earlier studies have shown that PUDV is an effective technique for fiber suspension velocity measurement (Xu and Aidun, 2001; Johan et al., 2001).

In the following sections, results obtained through PUDV measurement of flow of wood fiber suspension in a rectangular channel are presented. The flow characteristics of fiber suspension flow are studied and a model is presented to describe the turbulent velocity profile as a function of Reynolds number and fiber concentration.

2. Experimental setup

Fiber is dispersed in water at the desired concentration and pumped immediately through a Moyno pump into the flow loop where it is recirculated for 15 min to eliminate fluctuations due to initial transients. To reduce the pressure fluctuation in the flow loop, two surge suppressors are installed. The flow rate is measured by a Micro-Motion mass flow meter.

The fiber used in the experiments is natural flexible cellulous wood fiber with an average length of 2.3 mm and average diameter of about 35 μm. After the fiber is saturated with water, its density is similar to that of water. Therefore, the fiber is dispersed uniformly in the suspension without sedimentation during the entire experiment.

The experimental setup consists of a rectangular Plexiglas channel, shown in Fig. 1. One end of the channel is connected to a Plexiglas box 20 cm long, 12.7 cm wide, and 5.7 cm high. This box serves as a distributor to connect the feeding circular pipe with the rectangular channel. The fluid flows into the distributor from bottom and flows out through the side into the channel. The Plexiglas channel is 150 cm long, 5.08 cm wide and 1.65 cm high. At the end of the channel, as

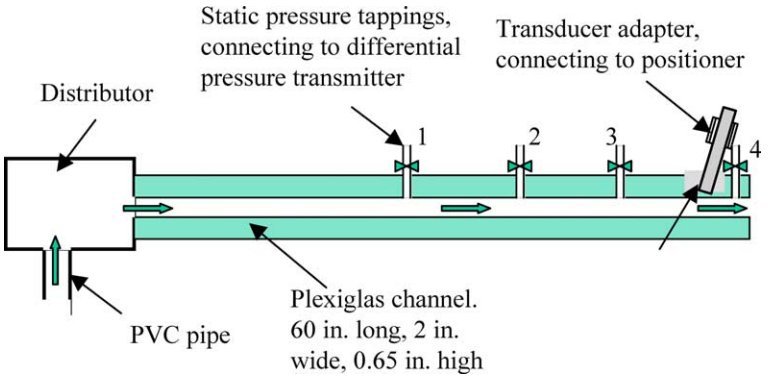

Fig. 1. Schematic of the fiber suspension flow in the channel.

shown in Fig. 1, a 2 cm diameter hole is cut in the center. The hole does not go all the way through the channel wall. It stops at 2 mm from the other side of the wall such that the wall thickness at the base of the hole reduces to 2 mm. During the velocity profile measurement, the ultrasonic transducer is inserted in this hole. Its position and inclination angle are adjusted by a precision X–Y–θ rotation positioner. The hole is filled with water to establish a coupling medium between the transducer and the Plexiglas wall (see Fig. 2).

The measuring system used for velocity profile measurements is pulsed ultrasonic Doppler velocimeter (Model 1032) with basic frequency of 4 MHz. The ultrasound transducer has an active diameter of 5 mm and the measuring volume is a thin-disc shape element with 5 mm diameter and 0.9 mm thick. The basic frequency is 4 MHz and the pulse repetition frequency ranges from 1812 Hz to 15.6 KHz depending on the magnitude of the velocity measured.

To characterize the fiber suspension flow, velocity profile measurements are carried out in a wide range of fiber concentrations and flow rates. The detailed test conditions at different flow rates and fiber concentrations are shown in Table 1, where the corresponding mean velocity, the Reynolds numbers based on water density and viscosity, and the parameter, nl^3, using average fiber length of $l = 2.3$ mm and aspect ratio of 60, are listed.

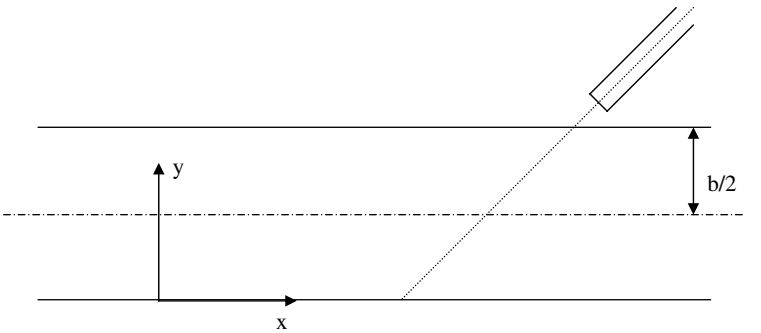

Fig. 2. Layout of the instrumentation and the channel coordinate system.

Table 1
Experiment conditions for velocity profile measurements

Flow rate ($m^3/s \times 10^{-3}$)	U_{avg} (m/s)	Re	Fiber concentration (%)/nl^3						
			0.05/0.33	0.1/0.67	0.15/1.0	0.3/2.0	0.5/3.3	0.75/5.0	1.0/6.7
0.14	0.16	2000		□	□	□	□	□	
0.21	0.23	3000		□	□	□	□	□	□
0.41	0.45	6000		□	□	□	□	□	□
0.82	0.91	12,000	□	□	□	□	□	□	□
2.52	2.90	37,000	□	□	□	□	□	□	□
4.10	4.56	60,000	□	□	□	□	□	□	□
5.05	5.60	73,000	□	□	□	□	□	□	□
6.31	7.00	92,000	□	□	□	□	□	□	□

3. Results and discussion

3.1. Effect of flow rate (Reynolds number) and fiber concentration on velocity profile

The two dominant parameters in this flow are the fiber concentration, presented here in terms of weight ratio, ϕ, or parameter, nl^3, and the Reynolds number, Re, based on the viscosity of water. In this study, Re represents a measure of the flow rate since the length scale, that is channel height, and the fluid viscosity remains constant. The experiments cover a range of fiber concentration from $\phi = 0.0$ to 1.0 (i.e., $nl^3 = 0$–6.7) and $Re = 2000$–92,000 from laminar to turbulent flow. The velocity is scaled with the velocity at the centerline, U_{max}, and length by the half channel height, $b/2$.

We are interested in capturing the variations in velocity profile as a function of Re and the fiber concentration. To that end, same data are plotted in Figs. 3 and 4 in terms of variations in Re and concentration. Here y is the distance from the channel wall and u is the mean stream-wise velocity profile. For comparison purposes, the velocity profile for single phase turbulent flow between infinite parallel planes (Pai, 1953), given by

$$\frac{u}{U_{max}} = 1 - 0.3293\left(1 - \frac{y}{b/2}\right)^2 - 0.6707\left(1 - \frac{y}{b/2}\right)^{32}, \quad (1)$$

is plotted in Figs. 3 and 4 along with the laminar parabolic velocity profile.

As shown in Fig. 3a and b, as Re increases, the velocity profile changes from laminar flow to turbulent transitional flow and finally to fully developed turbulent flow when nl^3 is less than or equal to 1. At this range of concentration, the presence of fibers has less effect on the flow behavior and the velocity profiles are similar to that of single phase flow. When nl^3 increases to 2.0 (Fig. 3c), the velocity profile depends strongly on the Reynolds number. An important characteristic is the formation of a blunt plug in the center of the channel at low flow rate ($Re = 2000$ and 3000). At higher flow rate, the plug is disrupted and the velocity profile becomes sharper ($Re = 6000$, 9000). With further increase in flow rate, this trend is reversed and velocity profiles become more flat as flow rate increases ($Re = 12{,}000$). At very high flow rate ($Re = 73{,}000$–92,000), velocity profiles overlap the fully developed turbulent velocity profile for single phase flow. At higher fiber

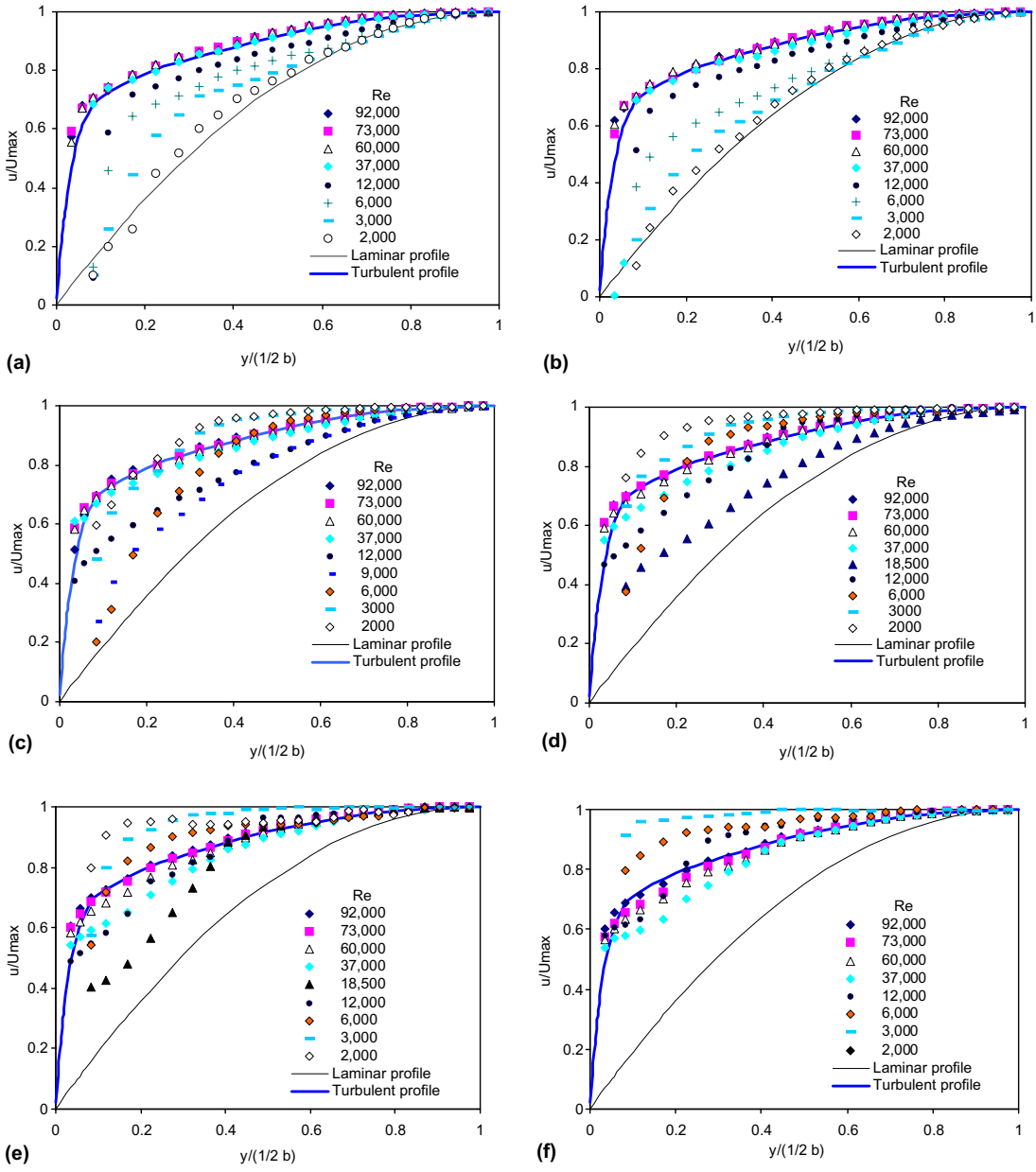

Fig. 3. Changes of velocity profile with flow rates for fiber suspension at different concentrations: (a) $nl^3 = 0.67$, (b) $nl^3 = 1.0$, (c) $nl^3 = 2.0$, (d) $nl^3 = 3.3$, (e) $nl^3 = 5.0$, (f) $nl^3 = 6.7$.

concentrations, the effect of Reynolds number on the shape of the velocity profile remains similar to the case with $nl^3 = 1.0$. The only difference is that with the increase of fiber concentration, the size of the central plug becomes larger at the same flow rate and the plug can be formed at higher Reynolds number (Fig. 3d–f).

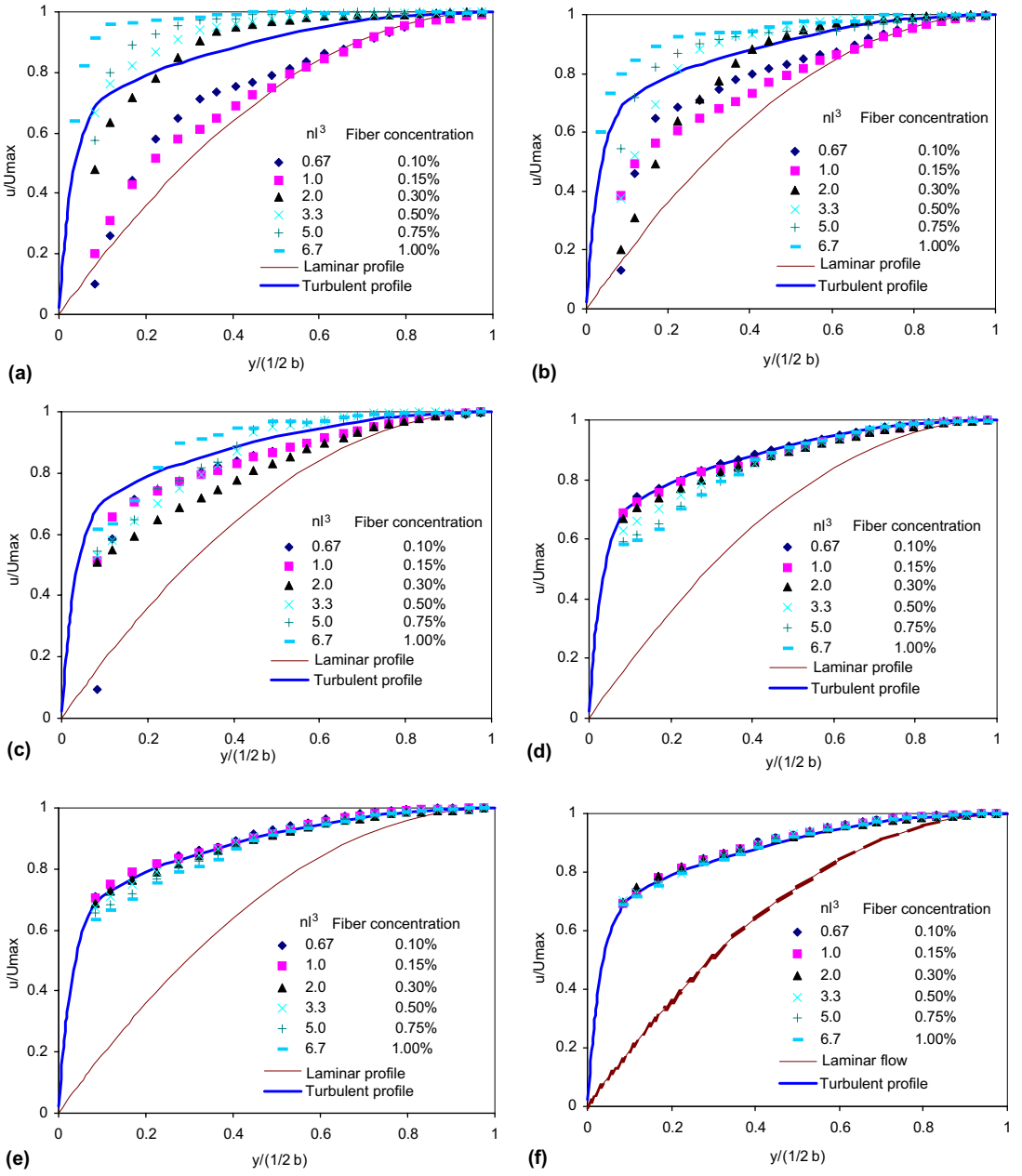

Fig. 4. Changes of velocity profile with fiber concentration at different Reynolds: (a) 3000, (b) 6000, (c) 12,000, (d) 37,000, (e) 60,000, (f) 92,000.

To show the effect of fiber concentrations on the flow behavior, the dimensionless velocity profiles in Fig. 3 are grouped by fiber concentration and redrawn in Fig. 4. The fiber concentration affects the shape of the velocity profile in two ways depending on the Reynolds number. At low

flow rate ($Re \leqslant 12{,}000$), the core part of the velocity profile becomes flat and a central plug forms for nl^3 greater than 1.0. At fixed flow rate, the plug size increases with the fiber concentration.

At a higher flow rate ($Re \geqslant 37{,}000$), fiber concentration does not have a significant effect on the shape of the velocity profile (Fig. 4d and e). However, the velocity profile becomes sharper when compared with the velocity profile of single phase flow at the same flow rate. The deviation from the velocity profile of single phase flow becomes larger as fiber concentration increases. Also, the deviation is higher at low flow rate. If the flow rate is high enough, the effect of fiber concentration becomes so small that there is virtually no difference between the velocity profiles of fiber suspension and that of single phase flow (Fig. 4f).

3.2. Turbulent intensity

There have been several attempts to measure turbulent fluctuation intensity in fiber suspension flow using impact probes and various diffusion techniques. However, because of the low frequency response of the measuring systems and heavy fiber buildup on the probe tip, these approaches can only measure large scale variations. A more promising approach is with the pulsed ultrasonic Doppler velocimetry, where instantaneous velocity at a relatively short sampling time can be measured. Therefore, the fluctuation of local instantaneous velocities will be reflected in the measuring results. It is possible to calculate the turbulent intensity based on fluctuations in the instantaneous velocity measurements. Fig. 5 shows the turbulent fluctuation intensity $\sqrt{\overline{u'^2}}/U$ throughout the channel in the turbulent regime with $Re = 12{,}000$–$92{,}000$. Here, $\sqrt{\overline{u'^2}}$ is the standard deviation of 256 instantaneous velocity measurements at a fixed position in the probe direction, and U is the average velocity at that point. The turbulent intensity measurements are for the component of velocity along the probe axis. The effect of the measurement volume and the relation between the various Reynolds stress components in the measured volume can be derived based on simple geometrical reasoning, as explained by Kikura et al. (2004).

In the laminar regime, the fluctuation intensity of the PUDV only represents the signal noise. For example, at $Re = 3000$ and fiber concentration 0.13 ($nl^3 = 1.0$), the signal fluctuation intensity is less than 0.005 everywhere except very close to the wall. The manner by which different factors affect the 'measured turbulent intensity' can be summarized as follows.

From the center of channel to the wall region, the turbulence intensity increases gradually. With the increase of fiber concentration, the turbulence intensity is reduced. With the increase of flow rate, the effect of fiber concentration on the turbulent intensity decreases gradually, and finally, if the flow rate is high enough, fiber concentration has almost no effect on turbulence intensity.

The turbulent intensity will be significantly lower in the region where a plug forms at the center of the channel (Fig. 5a). In the region outside the plug, the intensity is much higher than that of the plug region.

Because of the limitation of the measuring method, different sampling times are used when measuring velocity profiles at different flow rates. For example, the sampling time is 51.2 ms and 18.4 ms for the cases with $Re = 12{,}000$ and 92,000, respectively. Because of the large sample volume used during measurement (5 mm in diameter, 0.9 mm in length), the turbulent intensity in Fig. 5 represents the average velocity fluctuation in the sampled volume.

Results from the turbulent intensity measurements confirm the results reported by previous investigators (Daily and Bugliarello, 1958). The presence of fibers in the flow will reduce turbulent

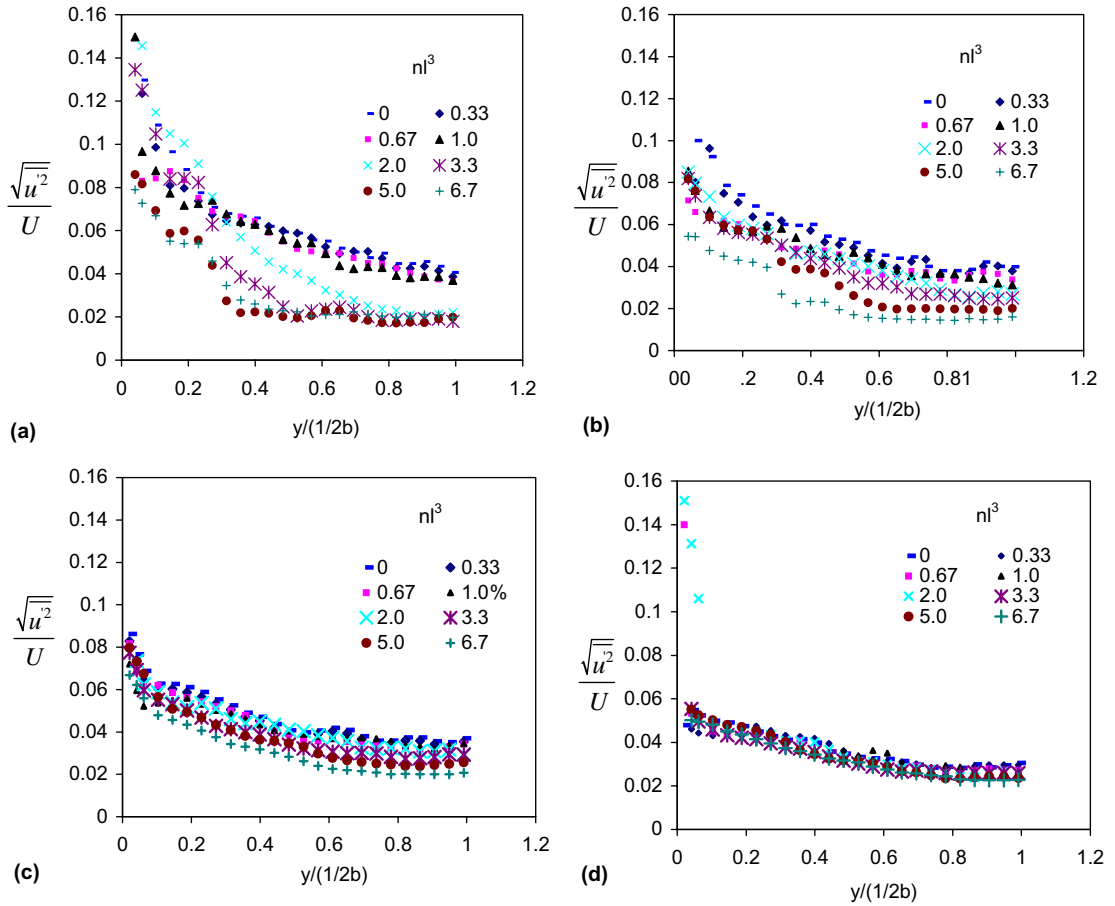

Fig. 5. Turbulent intensity of fiber suspension flow at different Reynolds number: (a) 12,000, (b) 37,000, (c) 60,000, (d) 92,000.

intensity. These results also provide insight into understanding the structure and flow mechanisms for fiber suspensions.

3.3. Characterization of fiber suspension flow

In their fundamental studies of fiber suspension flow, Forgacs et al. (1958) and Daily and Bugliarello (1958) showed that fiber suspensions exhibit three basic types of flow profiles—turbulent, mixed, and plug flow. In another study, Seely (1968) was unable to distinguish the velocity profiles he obtained for dilute fiber suspensions at high flow rates from those he obtained for pure water. He further divided the fully turbulent regime into two subregimes—"damped turbulent flow" and "Newtonian turbulent flow". However, the transitions between the different types of flow, especially from mixed flow to the damped turbulent flow, and then to fully turbulent flow have not been well established. In our experiments, five types of flow behavior have been

distinguished in the range of Reynolds numbers and fiber concentrations considered. These and their corresponding flow regimes in the fiber concentration and Reynolds number parameter space are shown schematically in Fig. 6a and b, respectively.

In the first type of flow (Fig. 6b, Region 1), the velocity profile is the same as the turbulent velocity profile for single phase Newtonian flow. The shape of the velocity profile will not change with Reynolds number and fiber concentration. Similarities in flow behavior between dilute suspension flows and single phase flow have been suggested and experimentally verified by Seely (1968). In the second type of flow (Fig. 6b, Region 2), the velocity gradient is larger than that of flow in Region 1. In this type of flow, velocity profile becomes gradually sharper by increasing the fiber concentration and/or decreasing the Reynolds number. With further increase of fiber concentration and/or decrease of Reynolds number, in Region 3, this trend reverses and the shape of the velocity profile becomes blunter. The flow behavior in Region 4 is termed 'mixed flow' in the literature (Forgacs et al., 1958; Daily and Bugliarello, 1958). This term is used here to describe the transition regime between plug flow (Region 5) and fully developed turbulent profile. It is simply the flow of a central plug region at uniform velocity with a turbulent flow region between the plug boundary and the channel wall. The plug region may be thought of as more or less a continuous fluid saturated fiber network, which is capable of supporting the shear stress applied to it. Since the transition from the third region to mixed flow is smooth, it is impossible to discern visually when the plug begins to form.

At low flow rate and high fiber concentration, in Region 5, the fibers in the suspension form interlocking coherent network in the entire flow field. Such networks have well-defined mechanical strength properties. A thin water layer exists between the plug and the wall.

The various flow profiles in Fig. 6a, and the corresponding flow regions in the parameter space of Fig. 6b, are determined based on the shape of the velocity profile and the manner in which the velocity profile changes with flow rate and fiber concentration. There is no obvious sharp transition point between different types of flow. With the increase of fiber concentration or decrease of flow rate, the flow gradually changes from the first type to the fifth type. The different types of

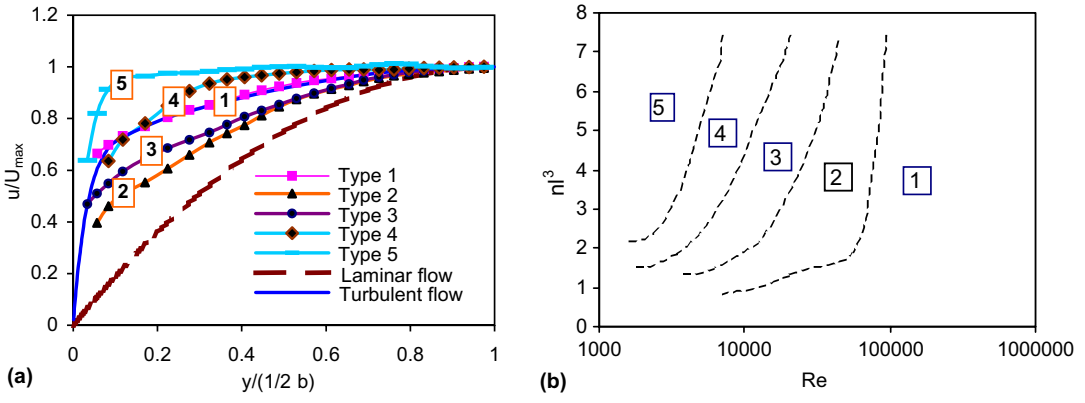

Fig. 6. Different types of velocity profiles and flow regions observed in the experiments: (a) different types of velocity profiles, (b) different types of flow regions.

flow behaviors and velocity profiles observed in this study can explain some of the inconsistent results reported in the literature. For example, the flow behavior in Region 3 is in agreement with Daily and Bugliarello's (1958) observation that velocity profile becomes blunter as fiber concentration increases. The flow behavior in Regions 1 and 2 are consistent with Seely's observation that the von Kármán constant increases in a systematic manner throughout the damped turbulent regime and approaches the single phase value at very high flow rate. Lee and Duffy (1976) investigated the velocity profiles of fiber suspension over a wide range of bulk velocities. They found that the fully turbulent velocity profiles become steeper as fiber concentration increases. The reduced local velocity (u^+ as defined in the next section) for fiber suspension in the turbulent flow regime is greater than that of single phase flow, such as water, under the same conditions. In the low flow rate turbulent regime, the von Kármán constant decreases with the flow rate, while at high flow rate regime the behavior is reversed. These two opposing observations are consistent with the flow behavior in Regions 2 and 3, respectively.

The variations in fiber suspension flow behavior and velocity profile with Reynolds number and fiber concentration can assist in understanding the complex internal flow mechanism of fiber suspensions. In the next section, we provide a model to predict the effect of fiber concentrations and Reynolds number on the velocity profile in turbulent fiber suspension flow.

3.4. Turbulent velocity profile for fiber suspension

Although the effect of fiber concentration and flow rate on the velocity profile has been reported in the literature, quantitative descriptions of this effect are not available. In order to quantify the effect of fiber concentrations and flow rates on fiber suspension flow, the velocity profiles ($Re \geqslant 37{,}000$, $nl^3 \geqslant 2.0$) are redrawn in the non-dimensional wall-layer coordinates, $u^+ = U/U_\tau$ and $y^+ = yU_\tau/\nu$, and shown in Fig. 7. Here, the wall shear velocity, U_τ, is defined as $(\tau_w/\rho)^{1/2}$, where ρ is the fluid density, and ν is the kinematic viscosity. The wall shear stress, τ_w, is obtained from the pressure drop measurements. The solid line in Fig. 7 is the theoretical velocity profile for single phase flow between infinite parallel plates, given by:

$$u^+ = \frac{1}{0.41}\ln(y^+) + 4.69. \tag{2}$$

Coles (1956) estimated the velocity profile by combining the log law and a wake function

$$u^+ = \frac{1}{\kappa}\ln(y^+) + B + \frac{\Pi}{\kappa} w\left(\frac{y}{0.5b}\right) \tag{3}$$

in which the von Kármán constant κ and B are determined by using the data measured in the region $y/(0.5b) < 0.15$, and the wake coefficient, Π, is calibrated with the data in the outer flow. Here, we will use the form of Eq. (3) to describe the velocity profile of turbulent fiber suspension flow. As shown in Fig. 7, the velocity profiles are overlapped to that of single phase flow in the inner wall region. Therefore, we can assume the value of κ and B will be the same as that for single phase flow—that is 0.41 and 4.69, respectively. In the outer wall region, however, the profiles deviate from Eq. (2) and the magnitude of the deviation can be described by the third term in Eq. (3).

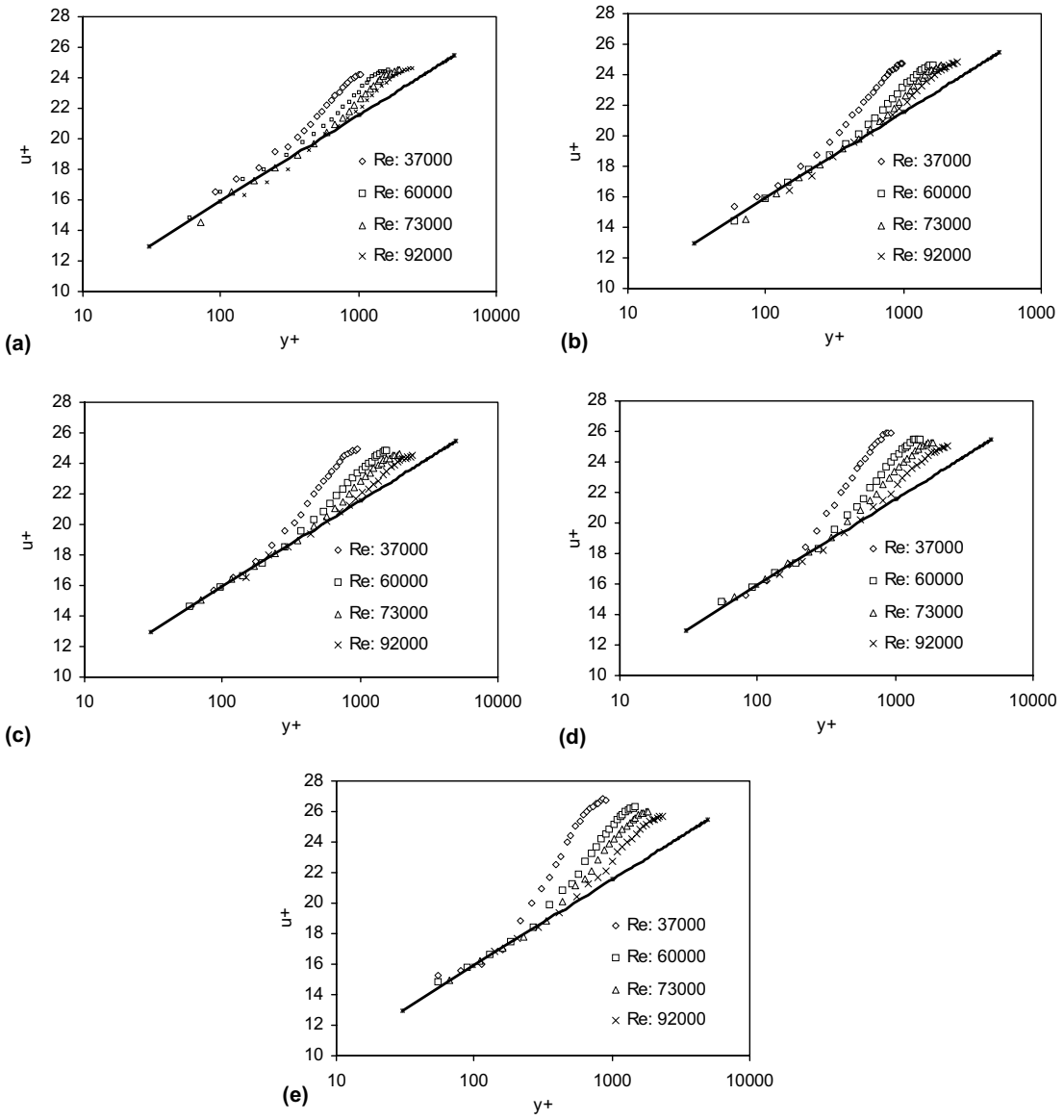

Fig. 7. The reduced velocity profiles: (a) $nl^3 = 1.0$, (b) $nl^3 = 2.0$, (c) $nl^3 = 3.3$, (d) $nl^3 = 5.0$, (e) $nl^3 = 6.7$.

From Fig. 7, it is clear that the deviation is a function of fiber concentration (nl^3), flow rate (Re) and position (y^+). Fig. 8 shows the deviation from log law at different Reynolds number and fiber concentration. Since the maximum deviation happens at $y/(0.5b) = 0.9$ in most of the velocity profiles, we use the following function to curve fit the deviation in Fig. 8:

$$f\left(Re, nl^3, \frac{y}{0.5b}\right) = \frac{\Pi}{\kappa} w\left(\frac{y}{0.5b}\right) = \frac{2\Pi}{\kappa} \sin^2\left(\frac{\Pi}{2}\frac{y}{0.5b}\frac{1}{0.9}\right). \tag{4}$$

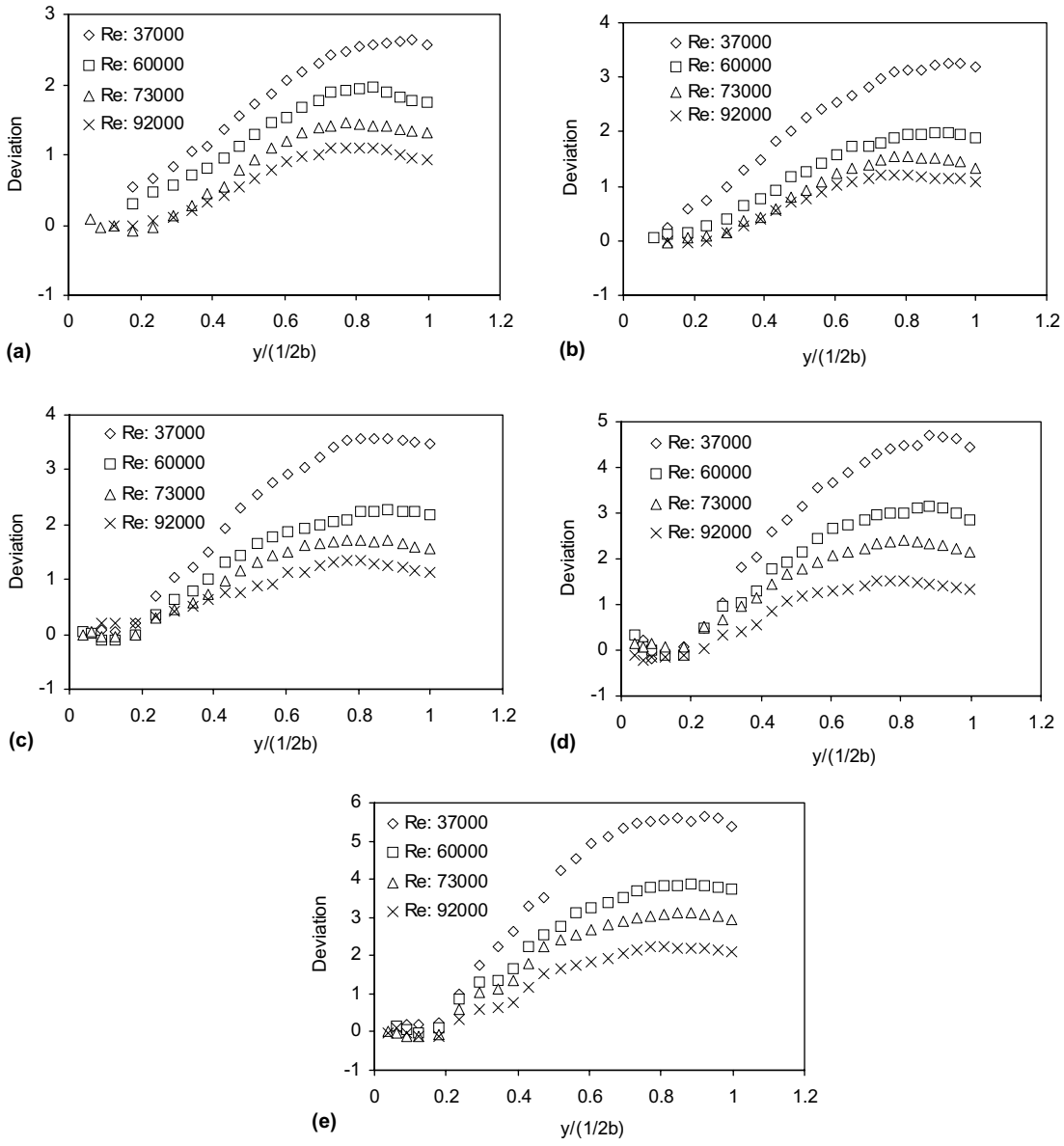

Fig. 8. The deviation of velocity profile of fiber suspension flow from log law at different fiber concentration and Reynolds number: (a) $nl^3 = 1.0$, (b) $nl^3 = 2.0$, (c) $nl^3 = 3.3$, (d) $nl^3 = 5.0$, (e) $nl^3 = 6.7$.

In the above equation, $w\left(\frac{y}{0.5b}\right)$ is a universal function independent of Reynolds number and fiber concentration. Π is a function of Reynolds number and fiber concentration—its value can be obtained through curve fitting for the deviation curve in Fig. 8. Fig. 9 presents the value of Π at different Reynolds number and fiber concentrations.

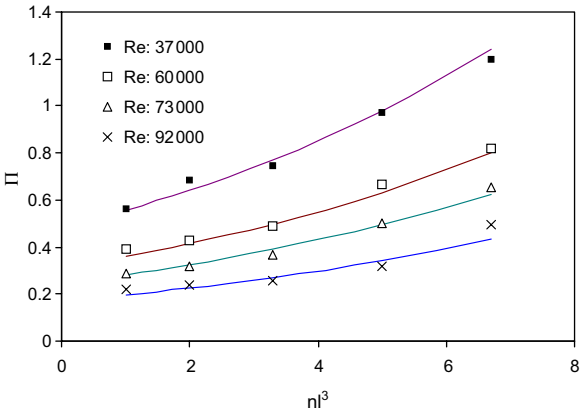

Fig. 9. The value of Π at different fiber concentrations and Reynolds number. The solid line is obtained using Eq. (5).

In order to describe Π in terms of Reynolds number and fiber concentration, the following equation is used for curve fitting the data points in Fig. 9:

$$\Pi = k_1 \exp(k_2(nl^3) - k_3 * Re). \tag{5}$$

Here, k_1, k_2, and k_3 are constants that could be obtained through curve fitting.

Rewriting the equation in the following form,

$$\ln(\Pi) = \ln(k_1) + k_2 * (nl^3) - k_3 * Re. \tag{6}$$

It can be shown from Eq. (6) that there is a linear relation between $\ln(\Pi)$, nl^3 and Re. The constants in this equation, obtained through linear regression for the data points in Fig. 9 are found to be $k_1 = 0.98$, $k_2 = 0.14$ and $k_3 = 1.9 * 10^{-5}$.

The solid line in Fig. 9 gives the predicted value of Π at different fiber concentrations and Reynolds number using Eq. (5) and the above constant values. As seen in this plot, the predicted Π value fits quite well with the experimental data.

Combining Eqs. (3)–(5), the velocity profile of fiber suspension flow could be rewritten in the following form,

$$u^+ = \frac{1}{0.41}\ln(y^+) + 4.69 + \frac{\Pi}{0.41}\sin^2\left(\frac{y}{0.9b}\pi\right) \tag{7}$$

where

$$\Pi = 0.98\exp(0.14nl^3 - 1.9 * 10^{-5} * Re) \tag{8}$$

Fig. 10 gives an example of the reduced velocity profiles at different Reynolds number ($nl^3 = 5.0$), where the predicted velocity profile based on Eqs. (7) and (8) are shown in the solid line. As shown in Fig. 10, the predicted velocity profiles correlate quite well with the experimental data. Therefore, the velocity profile of turbulent fiber suspension flow can be described by Eqs. (7) and (8). However, it should be noted that these two equations can only apply to the turbulent suspension flow in the turbulent regime.

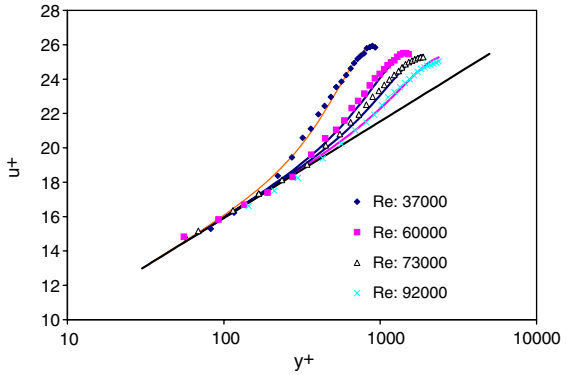

Fig. 10. The reduced velocity profile at $nl^3 = 5.0$. The dotted line is the experimental data and the solid line is the predicted velocity profile based on Eqs. (7) and (8).

3.5. Mechanism of fiber suspension flow

In fiber suspension flow, fibers tend to entangle with each other forming networks, sometimes referred to as flocs. Similar to the fiber concentration parameter nl^3, Kerekes and Schell (1992) defined a crowding factor N ($=5nl^3/\rho$, where ρ is the fluid density) to characterize the level of fiber–fiber contact, and the tendency of fibers to form flocs. At $N \approx 1$, fiber mobility is high and it is hard to form a floc. As N increases, fiber mobility decreases significantly and coherent flocs of sufficient strength form. This parameter is therefore a good practical measure of the tendency of the fiber suspension to form floc. In a turbulent fiber suspension flow, the amount of flocculation is determined by a dynamic equilibrium between the growth of flocs by collision processes and their breakdown by shear stress (Robertson and Mason, 1954). Fiber dispersion is found to be promoted by increasing the velocity gradient and by decreasing fiber concentration. On the other hand, fiber flocs are stated to affect momentum transfer in two opposing ways in the flow field: they tend to lower it by damping the turbulence of the suspending phase, and also tend to enhance the momentum transfer by providing a solid link between adjacent fluid layers (Norman et al., 1977). Because the local shear stress is related to the local velocity gradient through local momentum transfer, the forming of flocs will affect the momentum transfer, and thus affects the shape of the velocity profile.

In the first type of flow, as defined in the previous sections, because of the high shear stress and turbulent stress, it is difficult for fibers to interlock with each other, therefore less flocculation. In this type of flow, momentum transfer is dominated by turbulence and the addition of fibers to the suspension has less effect on the turbulent intensity, as proved in the previous measurements (Fig. 5d). Therefore, the velocity profile is about the same as that of single phase Newtonian fluid. In the second type of flow, part of the fibers in the suspension will interlock and form flocs with increasing fiber concentrations or decreasing shear stress (Reynolds number) as observed by Robertson and Mason (1954). The presence of fiber and formation of flocs will reduce the momentum transfer through decreasing turbulence intensity (as shown in Fig. 5) and, on the other hand, increase momentum transfer through fiber interlocking. The overall momentum transfer is

determined by the combination of these two effects. Reduction of momentum transfer caused by turbulence in the flow of the second type, when compared to single phase flow, is higher than the gain of momentum transfer caused by fiber interlocking. Therefore, the total momentum transfer is less than that of water flow, which leads to a sharper velocity profile in comparing with the velocity profile of a single phase flow.

With further increase of fiber concentration or decrease of flow rate, in the third type of flow, the contribution to the momentum transfer by fiber interlocking increases. The evidence of this change is that the central part of the velocity profiles becomes blunter with the increase of fiber concentration or decrease of flow rate.

The third type of flow is characterized by more significant influence of fiber network formation on momentum transfer than the effect of turbulence, when fiber concentration increases or flow rate decreases. This explains the blunter velocity profile at higher fiber concentration or lower flow rate.

In plug-turbulent mixed flow (Region 4), because of the low turbulence and shear stress, a fiber network forms in the center of the channel and provides a solid link between adjacent fluid layers. In this part of the flow, momentum transfer is dominated by the fiber interlocks. Outside the fiber network region, there is a layer of turbulent fiber suspension area and the turbulence intensity has been suppressed greatly (Fig. 5a) by the presence of fiber flocs. With further decrease of flow rate or increase of fiber concentrations, the size of the plug increases and eventually the plug will fill the entire flow region (Region 5).

4. Conclusions

Pulsed ultrasonic Doppler velocimetry has been used to measure the velocity profiles of fiber suspension flow in a rectangular channel. Five different types of flow behavior have been observed by varying the fiber concentration and the Reynolds number. In the first type, the velocity profile is the same as that of single phase flow. In the second type, the velocity profile becomes sharper with decreasing the flow rate and/or increasing the fiber concentration. With further decrease in flow rate and/or increase in fiber concentration, the velocity profile becomes blunter again in the third type of flow. At low flow rate and/or high fiber concentration, a plug will form in the center of the channel and fill the whole flow field if Reynolds number is low and/or fiber concentration is high enough.

The velocity profile of fiber suspension flow in turbulent flow can be predicted by a correlation given by

$$u^+ = \frac{1}{0.41}\ln(y^+) + 4.69 + \frac{\Pi}{0.41}\sin^2\left(\frac{y}{0.9b}\pi\right), \tag{9}$$

where b is the height of the channel and Π is the wake constant which is a function of fiber concentration nl^3 and Reynolds number Re.

The presence of fibers or fiber flocs in the suspension will reduce the turbulence intensity. This effect will decrease gradually when flow rate increases.

References

Andersson, S.R., Rasmuson, A., 2000. Flow measurement on turbulent fiber suspension by laser Doppler anemometry. AIChE J. 46, 1106–1119.

Batchelor, G.K., 1970. The stress system in a suspension of force free particles. J. Fluid Mech. 41, 813–829.

Batchelor, G.K., 1971. The stress generated in a non-dilute suspension of elongated particles by pure straining motion. J. Fluid Mech. 46, 813–829.

Coles, D., 1956. The law of the wake in the turbulent boundary layer. J. Fluid Mech. 1, 191–226.

Daily, J., Bugliarello, G., 1958. The effect of fibers on velocity distribution, turbulence and flow resistance of dilute suspensions. M.I.T. Hydrodynamics Laboratory Report, No. 30, Cambridge, MA, Massachusetts Institute of Technology.

Dong, S., Feng, X., Salcudenan, M., Gartshore, I., 2003. Concentration of pulp fibers in 3D turbulent channel flow. Int. J. Multiphase Flow 29, 1–21.

Forgacs, O.L., Robertson, A.A., Mason, S.G., 1958. The hydrodynamics behavior of paper-making fibers. Pulp Paper Mag. Canada 59, 117–127.

Hinch, E.J., Leal, L.G., 1976. Constitutive equations in suspension mechanics. Part 2. Approximate forms for a suspension of rigid particles affected by Brownian rotations. J. Fluid Mech. 76, 187–208.

Hookham, P.A., 1986. Concentration and Velocity Measurement in Suspensions Flowing through a Rectangular Channel. Ph.D. thesis, California Institute of Technology.

Johan, W., Johansson, M., Jeelani, S., Peter, F., Mats, S., Anne-Marie, H., 2001. In-line rheological measurement of complex model fluids using an Ultrasound UVP-PD based method. Annu. Trans. Nordic Rheol. Soc. 8/9, 128–130.

Kallio, G.A., Reeks, M.W., 1989. A numerical simulation of particle deposition in turbulent boundary layers. Int. J. Multiphase Flow 15, 433–446.

Kerekes, R.J., Garner, R.G., 1982. Measurement of turbulence in pulp suspensions by laser anemometry. Trans. Tech. Sect. CPPA 8, TR53.

Kerekes, R.J., Schell, C.J., 1992. Characterization of fiber flocculation by a crowding factor. J. Pulp Paper Sci. 18, 32–38.

Kikura, H., Yamanaka, G., Aritoma, M., 2004. Effect of measurement volume size on turbulent flow measurement using ultrasonic Doppler method. Exp. Fluids 36, 187–196.

Koh, C.J., Hookham, P., Leal, L.G., 1994. An experimental investigation of concentrated suspension flows in a rectangular channel. J. Fluid Mech. 266, 1–32.

Kroger, C., Drossinos, Y., 2000. A random-walk simulation of thermophoretic particle deposition in a turbulent boundary layer. Int. J. Multiphase Flow 26, 1325–1350.

Lee, P.F.W., Duffy, G.G., 1976. Velocity profiles in the drag reducing regime of pulp suspension flow. Appita 30, 219–226.

Li, T.Q., Seymour, R.L., Powell, M.J., McCarthy, J.K., McCarthy, K.L., Odlberg, L., 1994. Visualization of flow patterns of cellulose fiber suspensions by NMR imaging. AIChE J. 40, 1408–1411.

Mih, W., Parker, J.D., 1967. Velocity profile measurements and a phenomenological description of turbulent fiber suspension pipe flow. Tappi J. 50, 237–246.

Norman, B.G., Moller, K., Duffy, G.G., 1977. Hydrodynamics of papermaking fibers in water suspension. Fiber–water interactions in paper-making. The Brit. Paper Board Industry Federation 1, 195–246.

Olson, J.S., 1996. The Effect of Fiber Length on Passage through Narrow Apertures. Ph.D. thesis, University of British Columbia.

Pai, S.I., 1953. On turbulent flow between parallel plates. J. Appl. Mech. 20, 109–114.

Powell, R.L., Weldon, M., Ramaswamy, S., McCarthy, M., 1996. Characterization of pulp suspension. Tappi Engineering Conference, 525–530.

Rahnama, M., Koch, D., Shaqfeh, E., 1995. The effect of hydrodynamic interactions on the orientation distribution in a fiber suspension subject to simple shear flow. Phys. Fluids 7, 487–506.

Robertson, A.A., Mason, S.G., 1954. Flocculation in flowing pulp suspensions. Pulp and Paper Magazine of Canada, Convention Issue, 264–269.

Sanders, H.T., Meyer, H., 1971. Consistency distribution in turbulent flow of fiber suspensions. Tappi J. 54, 722–730.

Seely, T., 1968. Turbulent Pipe Flow of Dilute Fiber Suspensions. Ph.D. thesis, Institute of Paper Chemistry, Appleton, Wisconsin.

Shaqfeh, E.S.G., Fredrickson, G.H., 1990. The hydrodynamic stress in a suspension of rods. Phys. Fluids A 2, 7–24.

Shaqfeh, E.S.G., Koch, D.L., 1988. The effect of hydrodynamic interactions on the orientations of axisymmetric particles flowing through a fixed bed of spheres or fibers. Phys. Fluids 31, 728–743.

Steen, M., 1989. Turbulence structure in vertical pipe flow of fiber suspensions. Nordic Pulp Paper Res. J. 4, 244–252.

Takeda, Y., 1986. Velocity profile measurement by ultrasound Doppler shift method. Int. J. Heat Fluid Flow 7, 313–318.

Xu, H.J., Aidun, C.K., 2001. Characteristics of fiber suspension flow in a channel. 2001 Tappi Engineering and Finishing and Converting Conference, San Antonio, TX, September, 2001.

Yamamoto, S., Matsuoka, T., 1994. Viscosity of dilute suspensions of rod like particles: a numerical simulation method. J. Chem. Phys. 100, 3317–3324.